# Journal of Materials Chemistry

**PAPER**

# High performance encapsulant for light-emitting diodes (LEDs) by a sol–gel derived hydrogen siloxane hybrid

**Joon-Soo Kim, Seung Cheol Yang, Seung-Yeon Kwak, Yongwon Choi, Kyung-Wook Paik and Byeong-Soo Bae***

The hydrosilylation reaction is a dominant curing method for the light-emitting diode (LED) silicone encapsulant, which requires characteristics of high transparency, high refractive index, and thermal stability against the LED junction temperature. In this research, we synthesized a hydrogen containing oligosiloxane resin through non-hydrolytic sol–gel condensation. Methyldiethoxysilane (MDES) and diphenylsilanediol (DPSD) were used as precursors and a non-hydrolytic sol–gel condensation reaction was performed under acidic conditions. The synthesized hydrogen oligosiloxane resin was mixed with a phenyl and vinyl containing oligosiloxane (PVO) resin, which was prepared by a sol–gel condensation between vinyltrimethoxysilane (VTMS) and the DPSD. This blended solution was cured at 150 °C for 4 hours to complete the hydrosilylation reaction. The cured material (phenyl hybrimer) shows low shrinkage during the curing reaction and provides excellent transparency (∼90% at 450 nm) and thermal stability (440 °C) with a high refractive index ($n = 1.58$ at 632.8 nm).

## Introduction

LED (light-emitting diode) lighting is becoming an attractive replacement for the incandescent light bulb due to low power consumption, small size allowing application in specific narrow areas, and the use of non-toxic semiconductor materials.[1–5] As the application of LEDs is expanded on the strengths of the characteristics noted above, the requirements related to the LED encapsulant, a key component that occupies the dominant volume of LEDs, are also increasing. The LED encapsulant is an important element, as it covers and protects the LED chip and frangible wire and also keeps phosphors with high transparency to emit white light.[6–10]

Thermosetting epoxy resins such as diglycidyl ether of bisphenol-A or cycloaliphatic epoxy resins are generally used as encapsulation materials of LEDs due to their overall properties and cost. Unfortunately, these epoxy resins cannot sustain their transparency at the junction temperature.[11] They thermally decompose and easily lose their transparency, becoming yellowish and resulting in a serious decline of lighting performance. To address the yellowing issue, silicone has been considered as an encapsulation material due to its high thermal stability.[12] Phenyl groups generally approach the silicone material to increase the refractive index ($n = 1.53$), resulting in higher light extraction based on Snell's law. However, the phenyl groups are not stable at the junction temperature and therefore fail to satisfy the required thermal stability.[13] Specifically, the phenyl

radicals spread out due to cleavage from the linear siloxane backbone by thermal energy, generating a yellowish color.

Previously, we reported on a sol–gel derived siloxane hybrid material for use as an encapsulation material.[14] The branched linear structure of the phenyl-vinyl-oligosiloxane (PVO) resin increases the density of the fabricated material and prevents cleavage of phenyl groups from the siloxane backbone. As a result of the hydrosilylation reaction of the PVO resin with an excess amount of phenyltris(dimethylsiloxy)silane (PTDMSS), a material with excellent thermal resistance against yellowing (up to 200 °C) and a high refractive index could be achieved. It thus shows strong potential to be applied as an encapsulation material for LEDs. However, shrinkage during the thermal curing process due to the volatility of the PTDMSS monomer results in deformation of the initially designed optical shape. Another issue is the high curing temperature (180 °C) of the hydrosilylation reaction. This thermal heating could deteriorate the LED performance. In terms of practical application of an LED encapsulant, shrinkage, the issues of curing temperature and adhesion between the LED components are important, as well as thermal stability.

In this research, replacing PTDMSS as a cross-linker, we synthesized a Si–H containing oligosiloxane resin (HPO-resin) by sol–gel condensation between methyldiethoxysilane (MDES) and diphenylsilanediol (DPSD) to resolve the aforementioned issues related to encapsulation. The sol–gel condensation reaction was performed under acidic conditions with Amberlite as a catalyst.

Amberlite is known as an ion exchange catalyst and we accordingly sought to determine how ion species affect the sol–gel process. To this end, the sol–gel derived H-resin with

*Department of Materials Science and Engineering, KAIST, Daejeon, 305-701, Republic of Korea. E-mail: bsbae@kaist.ac.kr; Fax: +82 42 350 3310; Tel: +82 42 350 4119*

solvent-free PVO-resin was mixed in a 1 : 1 equivalent ratio with a Pt catalyst and the hydrosilylation reaction was processed at 150 °C for 4 hours. The final material, a phenyl hybrimer intended for application as a LED encapsulant, shows a high refractive index ($n$ = 1.58 at 632.8 nm), excellent transparency, and good thermal stability against yellowing (no color changes up to 150 °C over 1000 hours). Note that no commercial LED encapsulant materials reported to date can maintain transparency at 150 °C for more than 1000 hours.

## Experimental

### (1) Synthesis of the phenyl-vinyl-oligosiloxane resin (PVO-resin)

0.1 mol of vinyltrimethoxysilane (VTMS, Aldrich) and 0.1 mol of diphenylsilanediol (DPSD, Gelest) were used as precursors for a sol–gel condensation at 80 °C in a two-neck flask under stirring by a magnetic bar. Barium hydroxide monohydrate (BHM, Aldrich) in an amount of 0.1 mol% to the total precursors was used as a basic catalyst. $N_2$ gas was purged during the reaction to remove the methanol by-product. All procedures were performed inside a fume hood. The synthesized resin was filtered by a 0.45 μm Teflon filter.

### (2) Synthesis of the hydrogen-phenyl-oligosiloxane resins (HPO-resins)

0.1 mol of methyldiethoxysilane (MDES, Gelest) and 0.1 mol of DPSD were used as precursors for sol–gel condensation at 100 °C in a two-neck flask. 0.1 g/(0.1 mol of MDES) of Amberlite IRA 400 (Aldrich) and Amberlite IRC 76 (Aldrich) were used as acidic catalysts, respectively, to evaluate catalyst effects on the reaction. A water reflux tube was connected to one neck of the flask and the other neck was sealed by a rubber plug for the first 30 min of the reaction. The reflux tube and rubber plug were then removed and $N_2$ gas was purged to remove the by-product, ethanol. The total reaction time was 12 hours. All procedures were performed inside a fume hood. The synthesized resins were filtered by a 0.45 μm Teflon filter. Additionally, 0.2 mol of MDES and 0.3 mol of DPSD were used to optimize the composition of the precursors and the synthesis procedure was the same as described above.

### (3) Fabrication of the phenyl hybrimer from the hydrosilylation reaction between PVO-resin and HPO-resin

The synthesized PVO-resin and HPO-resin were mixed in a 1 : 1 equivalent ratio of vinyl (PVO-resin) to hydrogen–silicon. 1 wt% of platinum (0)–1,3-divinyl-1,1,3,3-tetramethyldisiloxane complex solution (Aldrich) (200 ppm of Pt) was added to the solution as a catalyst for the hydrosilylation reaction. The hydrosilylation reaction was performed under air at 150 °C for 4 hours to cure the solution.

### (4) Characteristics

The $^{29}Si$ nuclear magnetic resonance (NMR) spectra of oligosiloxane resins in 30 vol% of chloroform-d were recorded using a FT 600 MHz (Bruker Biospin, DMX600) instrument.

Chromium(III) acetylacetonate as a spin relaxation agent of silicon was added at a concentration of 30 mg $L^{-1}$. FT-IR (Fourier transform-infrared) spectroscopy (JASCO, FTIR 460 plus) and FT-Raman (Fourier transform-Raman) spectrometry were used to detect functional groups and the structure of the oligosiloxane resins. Optical transmittances and yellowness indices (ASTM D1925) were measured by a UV/Vis/NIR spectrophotometer (Shimadzu, UV-3101PC). A prism coupler (Metricon, 2010) was used to measure the refractive index at 632.8 nm. A shore durometer (Schmidt, HPSD) was used to measure the shore D hardness. Matrix assisted laser desorption ionization-time of flight (MALDI-TOF, Voyager-DE STR) was used to measure the distribution of the molecular weight of the oligosiloxane resins, and 2,5-dihydroxybenzoic acid was used as a matrix. A thermal gravimetric analysis (TGA, TA TGA 2050) was performed in air or $N_2$. A differential scanning calorimeter (DSC, Netzsch DSC 200 F3 Maia) was used to estimate the hydrosilylation reaction. The oxygen and water vapor permeability of the phenyl hybrimer (both sample size is $5 \times 5 \times 0.04$ $cm^3$) was characterized by permeability analysis (MOCON, OX-TRAN Model 2/21 and PERMATRAN-W MODEL 3/33, respectively). The oxygen permeability was measured at 23 °C and the water vapor permeability was measured at 37.8 °C with 100% RH (relative humidity).

## Results and discussion

### (1) The reaction mechanism of synthesis of HPO-resins by a sol–gel condensation

The platinum (Pt) catalyzed hydrosilylation reaction offers cross-linking among different chemical species utilized for synthesis of coupling agents, modification, and cross-linking polymers.[15–18] Previously, we used the hydrosilylation reaction to cure a vinyl containing sol–gel oligosiloxane resin with a Si–H containing monomer, phenyltris(dimethylsiloxy)silane (PTDMSS) monomer, for LED encapsulant application.

In this research, we prepared a Si–H containing cross-linker resin (Scheme 1) instead of the PTDMSS monomer by sol–gel condensation in order to address the shrinkage issue during the curing process. An important feature when using Si–H containing precursors is that the Si–H groups are very sensitive to moisture and are easily replaced with other chemical species or damaged. It was reported that hydrogen–silicon bonding is broken by the basic catalyst via the following chemical reaction (1).[19] Also, the water itself can hydrolyze the Si–H group.

$$\equiv Si-H + OH^- \rightarrow \equiv Si-OH + H^+ \qquad (1)$$
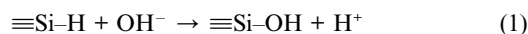
Acidic catalysts for sol–gel condensation were used to prevent these unexpected reactions. An acidic condition is also advantageous for the sol–gel condensation reaction between both D species (MDES, DPSD) considering the inductive effect. Under the acidic conditions, the reactivity of the sol–gel process (hydrolysis and condensation) increases depending on the substituent species, in the order of –R > –OR > –OH > –OSi. The basicity (electron providing) of the substitutes increases in this order under acidic conditions, accelerating the sol–gel process. Basically, in the sol–gel process, the synthesis of linear species is

This journal is © The Royal Society of Chemistry 2012

J. Mater. Chem., 2012, 22, 7954–7960 | 7955
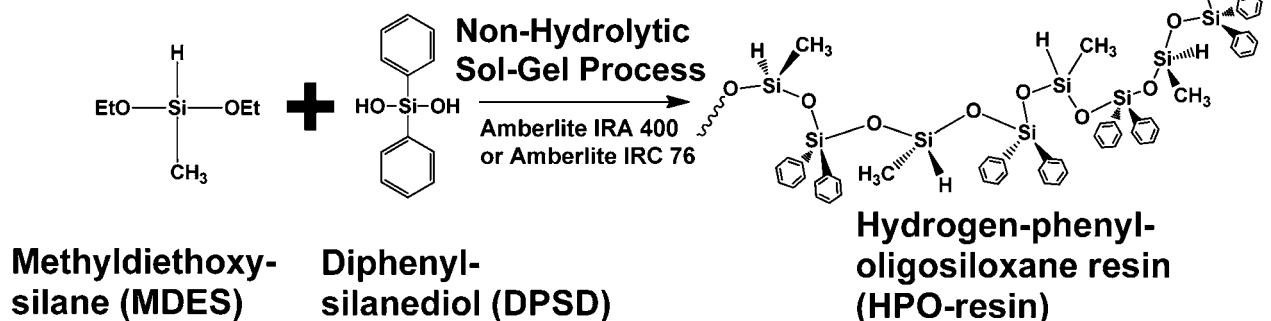
**Scheme 1** Synthesis of hydrogen-phenyl-oligosiloxane resin (HPO-resin) using methyldiethoxysilane (MDES) and diphenylsilanediol (DPSD) by a non-hydrolytic sol–gel process with Amberlite IRA 400 or Amberlite IRC 76.
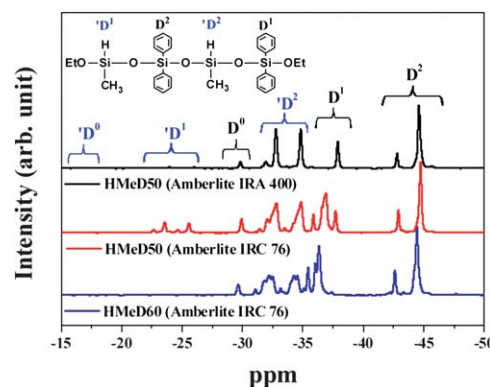
preferred under the acidic conditions based on the inductive effect,[20] because the partial charge of the alkoxy (–OR) group (in the case of MDES, ethoxy group) in the terminal side of the molecule is more negative than that of the internal alkoxy group. Thus, the ease of protonation of the alkoxy group at the terminal side is higher than the internal group, resulting in the formation of linear species.

Amberlite IRA 400 and Amberlite IRC 76 are known as an anion exchange resin and a cation exchange resin, respectively, and both resins show a weak acidic condition in solution. Because the catalysts are solid bead type, they can be easily filtered by a 0.45 μm Teflon filter. While the usual role of Amberlite is to exchange target ionic species in solution, it was used as an acidic catalyst in this research. The key difference between the two Amberlites is that the containing ion species in Amberlite IRA 400 and Amberlite IRC 76 are $Cl^-$ and $H^+$, respectively. We discuss how these ionic species affect the sol–gel condensation and which catalyst is suitable for preparing a Si–H containing oligosiloxane resin for the hydrosilylation reaction.

As noted above, water should be avoided in order to keep the Si–H group active for the hydrosilylation reaction. Amberlite is a suitable catalyst since it does not contain water. Also, the hydroxyl group (–OH) in the DPSD makes it possible to perform non-hydrolytic sol–gel condensation without adding water to the precursors. Table 1 indicates the synthesized hydrogen-phenyl-oligosiloxane resin (HPO-resin) compositions and degree of condensation (DOC) depending on the adopted catalysts. The DOC was calculated by the following eqn (2) based on a $^{29}Si$ NMR spectra analysis in Fig. 1.[21] The chemical shifts of the Si atom in the HPO-resin depend on its bonding structures.
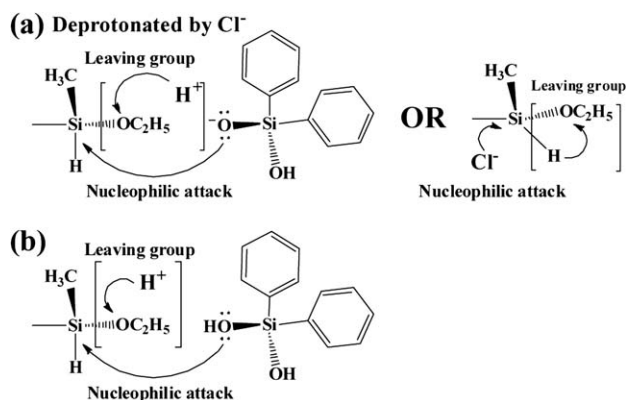


**Fig. 1** $^{29}Si$ NMR spectra of the hydrogen-phenyl-oligosiloxane resins (HPO-resin 50 using Amberlite IRA 400 or Amberlite IRC 76 and HPO-resin 60 Amberlite IRC 76).

$$\text{Degree of condensation} = \frac{D^1 + 2D^2}{2(D^0 + D^1 + D^2)} \times 100 \quad (2)$$

The DOC of each HPO-resin has a broad distinction depending on the catalyst (Amberlite IRA 400 or Amberlite IRC 76). The $Cl^-$ ions in Amberlite IRA 400 act similar to $HO^-$, thereby influencing the condensation reaction.[22] Regarding this behavior of halide species in the sol–gel process, it was also reported that the addition of $F^-$ decreases the gel time, thereby increasing the condensation reaction.

As shown in Scheme 2, the $Cl^-$ accelerates the nucleophilic attack of DPSD to the MDES by deprotonation of the hydroxyl group in DPSD, resulting in 91.6% DOC after the reaction. In contrast, the HPO-resin using Amberlite IRC 76 shows a low DOC value of 79.4% due to the relatively low reactivity of the condensation reaction under the acidic conditions. The mechanisms of the sol–gel condensation for each Amberlite are indicated in Scheme 2.

Even though the condensation reaction is preferred using Amberlite IRA 400 due to $Cl^-$, it negatively affects the Si–H groups. $Cl^-$ not only supports nucleophilic attack by deprotonation, it also damages the Si–H group by deprotonation of hydrogen bonding of the silicon atom, as shown in Scheme 2(a). Furthermore, $Cl^-$ can attach to the hydrogen deactivated Si–H group for the hydrosilylation reaction.

**Table 1** Degree of condensation (%) of the HPO-resins depending on precursor compositions and catalysts

| HPO-resin | MDES (mol%) | DPSD (mol%) | DOC (%) | Catalyst (ionic species) |
|---|---|---|---|---|
| HPO-resin 50 | 50 | 50 | 91.5 | Amberlite IRA 400 ($Cl^-$) |
| HPO-resin 50 | 50 | 50 | 79.4 | Amberlite IRC 76 ($H^+$) |
| HPO-resin 60 | 40 | 60 | 81.7 | Amberlite IRC 76 ($H^+$) |

**Scheme 2** Mechanisms of the non-hydrolytic sol–gel condensation between MDES and DPSD. (a) Amberlite IRA 400 (Cl⁻) and (b) Amberlite IRC 76 (H⁺) were used as catalysts for the reaction.
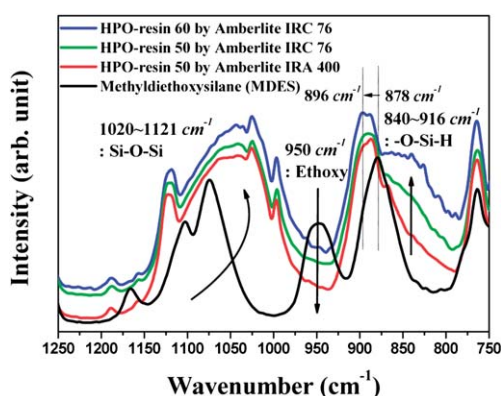


**Fig. 2** FT-IR spectra of HPO-resins prepared by non-hydrolytic sol–gel condensation. Si–O–Si networks (at 1020–1121 cm⁻¹) were formed as a result of sol–gel condensation. Also, the ethoxy (–OCH₂CH₃) peak (at 950 cm⁻¹) in the MDES was removed after the reaction. The peaks at 840–916 cm⁻¹ are attributed to the formation of –O–Si–H (bending vibration mode).

The peaks at 840–916 cm⁻¹ (bending vibration) of the FT-IR analysis shown in Fig. 2 indicate the –O–Si–H bond formed by the sol–gel condensation reaction.[23] The peak at 878 cm⁻¹ is induced by the initial state of MDES. Another peak at 896 cm⁻¹ from synthesized HPO-resins indicates also the O–Si–H group but they are shifted from 878 cm⁻¹ due to different pendant groups generated by the synthesis. The broad shoulder peaks around at 840 cm⁻¹ appear after the reaction and these groups highly affect the cross-linking for the hydrosilylation reaction. Si–O–Si networks (at 1020–1121 cm⁻¹) generated and the ethoxy (–OCH₂CH₃) peak (at 950 cm⁻¹) in the MDES was removed after the reaction.

The intensity at 840–916 cm⁻¹ started to increase after the reaction (there are no shoulder peaks in the initial MDES before the reaction) and it is higher when Amberlite IRC 76 was used as a catalyst while the intensity is lower when Amberlite IRA 400 was used, indicating the damage of the Si–H groups.

The direction given by an arrow in Fig. 3 indicates that the exothermic reaction of the hydrosilylation reaction is accelerated when Amberlite IRC 76 was used for synthesis of HPO-resin 50. The red line (Amberlite IRC 76) in the 120–245 °C range represents more hydrosilylation reaction is processed than the
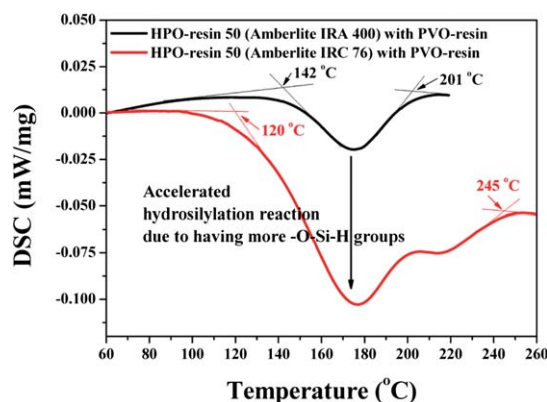


**Fig. 3** DSC spectra of HPO-resins with PVO-resin for the hydrosilylation reaction. HPO resin prepared using the Amberlite IRC 76 catalyst shows more exothermal energy than that prepared using the Amberlite IRA 400 catalyst.

black line (Amberlite IRA 400) in the 142–201 °C range. It confirms Amberlite IRC 76 is a proper catalyst for the synthesis compared to Amberlite IRA 400. We chose Amberlite IRC 76 as a catalyst for the synthesis on the basis of the results of the above analysis.

The chemically designed phenyl hybrimer with the synthesized HPO-resin with PVO-resin is described in Scheme 3. The hybrimer stands for an organic–inorganic hybrid material which complementarily enhances both organic and inorganic properties.[24,25] To achieve the desired chemical structure by cross-linking both resins through the hydrosilylation reaction, both the activity of Si–H groups mentioned thus far and the functionality of the Si–H groups on a molecule of the HPO-resin are required. Research on the relationship between the distribution of the number of functional groups (functionality) on the polymers and cross-linking has been carried out.

$$x_c = \frac{1}{\left[ r \left( f_{vinyl} - 1 \right) \left( f_{hydrogen-silicon} - 1 \right) \right]^{1/2}} \qquad (3)$$
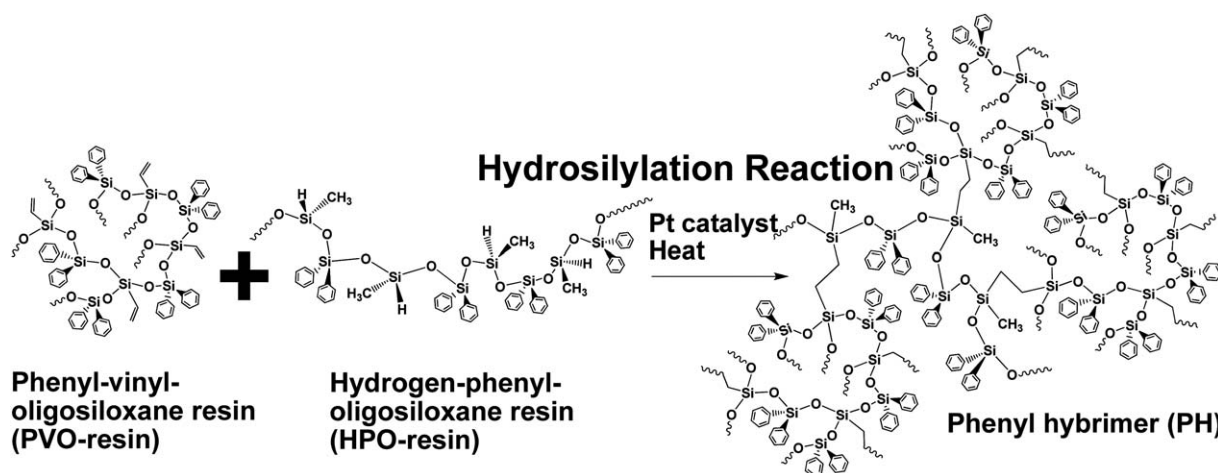
As delineated in eqn (3), based on the Flory–Stockmayer theory, the cross-linking point ($x_c$) depends on the functionality ($f_{vinyl}$ or $f_{hydrogen-silicon}$) of the vinyl or the hydrogenosilane (Si–H) groups on oligosiloxane resins.[26]

The low value of $x_c$ derived from a high $f$ indicates that there are many opportunities to cross-link each molecule as well as to increase the density of the cross-linking.

Thus, the functionality of the HPO-resin should be as high as possible for optimal cross-linking of the sol–gel derived oligosiloxane resins. The $r$ indicates the ratio of a hydrogen–silicon group to a vinyl group ($r = 1$). The functionality of the vinyl ($f_{vinyl}$) or the hydrogen–silicon ($f_{hydrogen-silicon}$) group can be calculated by the following eqn (4) and $A_f$ represents the number of molecules with functionality ($f$).

$$f_{vinyl} \text{ or } f_{hydrogen-silicon} = \frac{\sum_f f^2 A_f}{\sum_f f A_f} \qquad (4)$$

The functionalities of Si–H in the HPO-resin 50 and HPO-60 resin are approximately 2.8 and 5.0, respectively using eqn (4), based on results from a MALDI-TOF analysis of both resins, as

## Hydrosilylation Reaction



**Phenyl-vinyl-oligosiloxane resin (PVO-resin)**

**Hydrogen-phenyl-oligosiloxane resin (HPO-resin)**

Pt catalyst Heat

**Phenyl hybrimer (PH)**

**Scheme 3** Fabrication of the phenyl hybrimer (PH) through a hydrosilylation reaction between the sol–gel derived PVO-resin and HPO-resin.
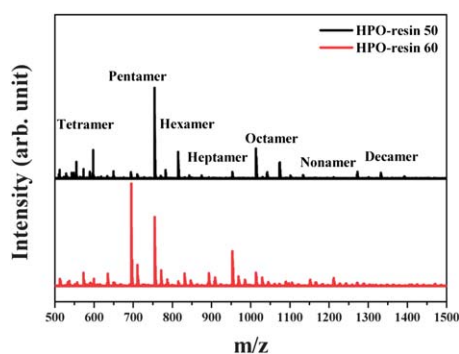


**Fig. 4** MALDI-TOF spectra of HPO-resin 50 and HPO-resin 60 using Amberlite IRC 76.

shown in Fig. 4.[27] Since the intensity of a MALDI-TOF is proportional to the molar amount of each molecular species, we can estimate the molecular weight of each species. And their individual functionality can be also estimated depending on molecular species.

As the DPSD content increases from 50 mol% (HPO-resin 50) to 60 mol% (HPO-resin 60), the DOC also becomes high and the functionality (Si–H) induced by MDES in the sol–gel derived oligosiloxane molecule becomes high enough to carry out the hydrosilylation reaction to increase cross-linking density. Thus, the HPO-resin 60 composition is appropriate for cross-linking with the PVO-resin. The functionality of the vinyl group in the PVO-resin is roughly 2.8, as obtained by eqn (4).

As seen in DSC curves shown in Fig. 5, an increase of the Pt catalyst accelerates the hydrosilylation reaction resulting in low onset temperature. The onset temperature is reduced from 145 °C to 75 °C since the Pt catalyst was added to resin gradually from 10 ppm to 200 ppm. Enough Pt catalyst scales the activation energy barrier down and consequently the curing temperature can be lowered.[28]

An excess amount of the Pt catalyst should be avoided, however, in terms of yellowing due to high light absorption of the metal catalyst. Thus, the amount of the Pt catalyst also has to be considered as well as the reactivity between the PVO-resin and the HPO-resin. 200 ppm is a suitable value for an adequate
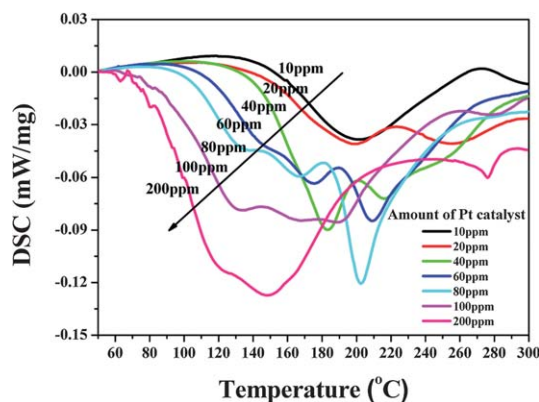


**Fig. 5** DSC spectra of mixture resins of HPO-resin 60 using Amberlite IRC 76 and PVO-resin with various amounts of Pt catalyst (10/20/40/60/80/100/200 ppm).

hydrosilylation reaction without any yellowing behavior. Also, in order to satisfy the condition of curing at 150 °C to prevent the LED components from thermal degradation, a sufficient amount of catalyst is similarly required.

The curing conditions of the phenyl hybrimer were optimized according to the following procedure. The mixture of the PVO-resin and HPO-resin (1 : 1 equivalent ratio) with the Pt catalyst (200 ppm) was prepared by curing by means of the hydro-silylation reaction at 150 °C for 4 hours.

### (2) The characteristics of the phenyl-hybrimer

As shown in Fig. 6, the isothermal TGA of each mixture resin, that is, the PVO-resin with HPO-resin and the PVO-resin with PTDMSS (previous resin composition), was performed at 150 °C and 180 °C, respectively. The previous mixture resin showed almost 15% weight loss from the initial state, whereas the mixture resin of the PVO-resin with HPO-resin shows approximately 1% weight loss. The inset images in Fig. 6 confirm that the HPO-resin exhibits low shrinkage and retains its initial flat surface after the curing process. The inset image (c) in Fig. 6 presents each mixture resin encapsulated LED after the curing process. Note that the difference between the two resins can be clearly
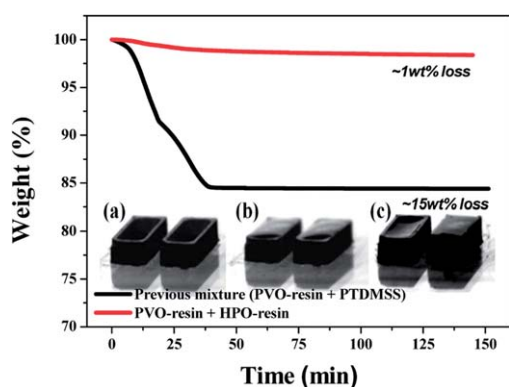
**Fig. 6** Isothermal TGA analysis of a mixed resin of PVO-resin with HPO-resin 60 and a previous mixed resin (PVO-resin + PTDMSS) at 150 °C and 180 °C, respectively. The inset image indicates the influence of weight loss during the hydrosilylation reaction on the shrinkage. (a) The empty LED cups. (b) Full LED cups with each mixed resin (left: PVO-resin + PTDMSS, right: PVO-resin + HPO-resin 60). (c) Encapsulated LED cups by each mixed resin after the curing process.

seen. The left image, the previous mixture resin, reveals significant shrinkage compared with the mixture of the PVO-resin and the HPO-resin, although the initial shapes before the curing process are maintained, as shown in inset image (b) in Fig. 6.
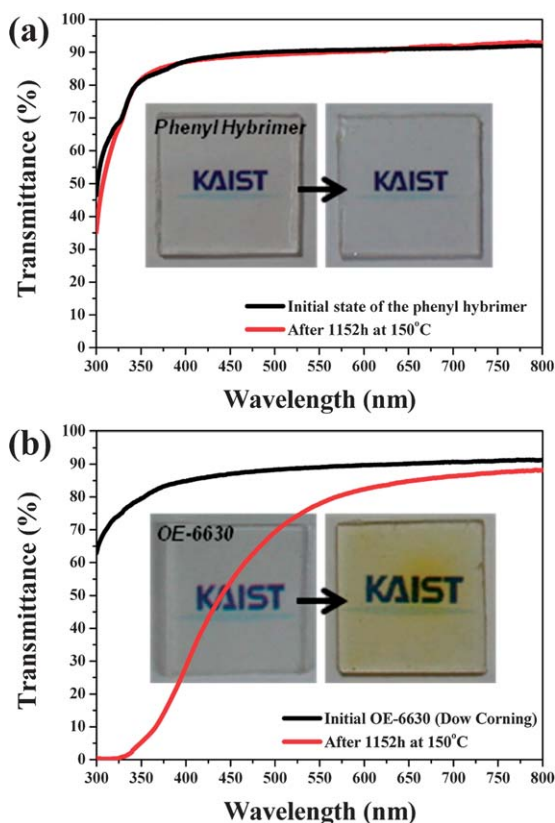


**Fig. 7** Comparison of transmittance (%) spectra before and after the thermal aging test at 150 °C for 1152 hours depending on wavelength (nm) is plotted. (a) The bulk (sample size: $2 \times 2 \times 0.2$ cm³) of the phenyl hybrimer by the PVO-resin and the HPO-resin 60. (b) The bulk (sample size: $2 \times 2 \times 0.2$ cm³) of OE-6630 (Dow Corning). The inset images represent the pictures before and after the thermal aging test.

The transmittances (%) for the case of 2 mm thick bulk samples of the phenyl-hybrimer and OE-6630, which is the model nomenclature of a commercial LED encapsulant (Dow Corning), were measured before and after a thermal aging test at 150 °C for 1152 hours (48 days), and the results are shown in Fig. 7. The transmittance (%) at 450 nm of the phenyl-hybrimer before (89.2%) and after (88.5%) the thermal aging test is similar, whereas the difference in the transmittance (%) is large in the case of the OE-6630 sample. The OE-6630 shows 87.0% transmittance at 450 nm at the initial state, but the transmittance decreases to 54.0% after the thermal aging test. This degradation behavior is also demonstrated by measuring the yellowness index (YI) based on ASTM, D1945.

The YI of the OE-6630 is 5.4 at the initial state and increases to 26.6 after the thermal aging test ($\Delta$YI = 21.2). In contrast, there is almost no change of the YI detected before (1.82) and after (1.85) the thermal aging test ($\Delta$YI = 0.03). The results from the thermal aging test indicate excellent thermal stability of the phenyl hybrimer against yellowing.

**Table 2** Characteristics of the phenyl hybrimer

| Property | Unit | Value |
| --- | --- | --- |
| Refractive index | $n$ (at 632.8 nm) | 1.5788 |
| Transmittance | % (at 450 nm) | 89.2 |
| 5 wt% loss temperature[a] | °C (in $N_2$) | 441.1 |
| Hardness | Shore D | 60 |
| $O_2$ permeability | cm³ mil m⁻² day⁻¹ | $3.32 \times 10^3$ |
| Water vapor permeability | g mil m⁻² day⁻¹ | $1.55 \times 10^2$ |

[a] Measured by TGA with a heating rate of 5 °C min⁻¹.
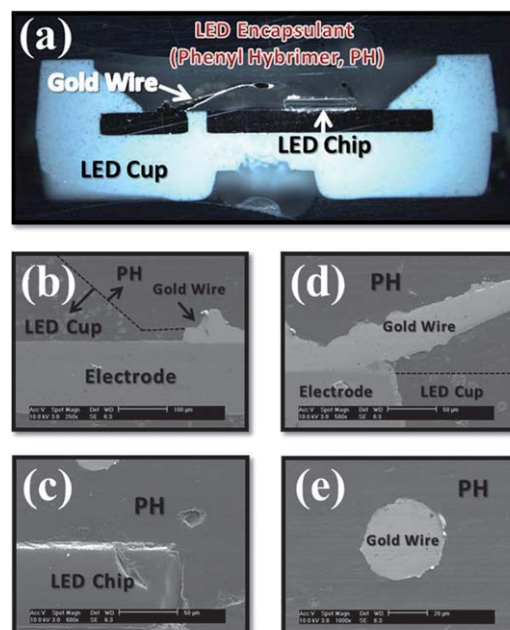


**Fig. 8** (a) A microscope image of the cross-sectional view of the phenyl hybrimer encapsulated LED is shown. SEM images of the interfaces between the phenyl hybrimer encapsulated in the LED and (b) the LED cup, (c) the LED chip and (d and e) gold wire were taken.

The overall characteristics of the phenyl hybrimer are also summarized in Table 2 including low oxygen and water vapor permeability compared to general polysiloxane such as PDMS (polydimethylsiloxane, the PDMS has high oxygen and water vapor permeability as $1.6 \times 10^{24}$ cm$^3$ mil m$^{-2}$ day$^{-1}$ and $3.14 \times 10^3$ g mil m$^{-2}$ day$^{-1}$, respectively).[29,30]

The optimized phenyl hybrimer was used to encapsulate a LED package. Microscope and SEM images of the phenyl hybrimer encapsulated LED in Fig. 8(a)–(e) reveal good adhesion of the phenyl hybrimer to the LED components, such as LED cup, LED chip, and gold wire. The interfaces between each component are filled with the phenyl hybrimer without leaving any empty space.

## Conclusions

We previously demonstrated a PVO-resin can be cross-linked with Si–H containing species through a hydrosilylation reaction and the product yielded by this reaction shows high transparency with excellent thermal stability. In this research, a Si–H group functionalized oligosiloxane resin (HPO-resin) was successfully synthesized using MDES and DPSD by means of a non-hydrolytic sol–gel process for use as a shrinkless and high refractive index cross-linker. In contrast to other condensation reactions in the sol–gel process, preparation of the Si–H containing chemical compounds should be performed under acidic conditions in order to protect the Si–H from deprotonation.

The phenyl hybrimer obtained by using the PVO-resin with HPO-resin shows high transparency (∼90%) at the visible range and a high refractive index ($n = 1.58$), as well as excellent thermal stability against yellowing. There was almost no color change after a thermal aging test at 150 °C for 48 days, whereas the commercial LED encapsulant material ($n = 1.53$) lost transparency via yellowing during an identical thermal aging test. We demonstrated that sol–gel derived oligosiloxane resins can be successfully applied as an LED encapsulant.

## Acknowledgements

## Notes and references

1 P. Patel, *MRS Bull.*, 2011, **36**, 678.
2 E. Tekin, H. Wijlaars, E. Holder, D. A. M. Egbe and U. S. Schubert, *J. Mater. Chem.*, 2006, **16**, 4294.
3 A. Tsami, X. Yang, F. Galbrecht, T. Farrell, H. Li, S. Adamczyk, R. Heiderhoff, L. J. Balk, D. Neher and E. Holder, *J. Polym. Sci., Part A: Polym. Chem.*, 2007, **45**, 4773.
4 A. Tsami, X. Yang, T. Farrell, D. Neher and E. Holder, *J. Polym. Sci., Part A: Polym. Chem.*, 2008, **46**, 7794.
5 I. Kanelidis, Y. Ren, V. Lesnyak, J.-C. Gasse, R. Frahm, A. Eychmüller and E. Holder, *J. Polym. Sci., Part A: Polym. Chem.*, 2011, **49**, 392.
6 S. D. Lester, J. N. Miller and D. B. Roitman, *US Pat.*, 577433, 1998.
7 N. R. Taskar, V. Chabra, D. Dorman and S. P. Herko, *WO Pat.*, 2005027576, 2005.
8 J. C. Huang, Y. P. Chu, M. Wei and R. D. Deanin, *Adv. Polym. Technol.*, 2004, **23**, 298.
9 A. W. Norris, M. Bahadur and M. Yoshitake, *Proc. SPIE–Int. Soc. Opt. Eng.*, 2005, **5941**, 594115-1.
10 T. Eiichi and M. Takashi, *JP Pat.*, 2005272697, 2005.
11 L. Bourget, R. J. P. Corriu, D. Lecercq, P. H. Mutin and A. Vioux, *J. Non-Cryst. Solids*, 1998, **242**, 81.
12 S. Katayama, N. Yamada, Y. Shibata and K. Nosa, *J. Ceram. Soc. Jpn.*, 2003, **111**, 391.
13 J. D. Macjenzue, *Ultrastructure Processing of Ceramics, Glasses and Composite*, ed. L. L. Hench and D. R. Ulrich, Wiley, NY, 1984.
14 J. S. Kim, S. C. Yang and B. S. Bae, *Chem. Mater.*, 2010, **22**, 3549.
15 *Comprehensive Handbook on Hydrosilylation*, ed. B. Marciniec, Pergamon Press, Elmsford, NY, 1992, ch. 3.
16 (a) J. F. Harrod and A. J. Chalk, *J. Am. Chem. Soc.*, 1964, **86**, 1776; (b) J. F. Harrod and A. J. Chalk, *J. Am. Chem. Soc.*, 1965, **87**, 16; (c) J. F. Harrod and A. J. Chalk, *J. Am. Chem. Soc.*, 1966, **88**, 2391.
17 (a) V. O. Reikhsfel'd and M. I. Astrakjanov, *Zh. Obshch. Khim.*, 1970, **40**, 699; (b) V. O. Reikhsfel'd and G. N. Koroleva, *Zh. Obshch. Khim.*, 1966, **36**, 1474.
18 H.-J. Egelhaaf, E. Holder, P. Herman, H. A. Mayer, D. Oelkrug and E. Lindner, *J. Mater. Chem.*, 2001, **11**, 2445.
19 T. A. C. Flipsen, H. Derks, V. D. Vegt, A. J. Pennings and G. Hadziioannou, *J. Polym. Sci., Part A: Polym. Chem.*, 1997, **35**, 41.
20 C. J. Brinker and G. W. Scherer, *Sol–Gel Science*, Academic Press, CA, 1990, ch. 3.
21 W. S. Kim, R. Houbertz, T. H. Lee and B. S. Bae, *J. Polym. Sci., Part B: Polym. Phys.*, 2004, **42**, 1979.
22 R. J. P. Corriu and J. C. Young, *The Chemistry of Organic Silicon Compounds*, ed. S. Patai and Z. Rappoport, Wiley, NY, 1989, ch. 20.
23 C. Marcolli and G. Calzaferri, *J. Phys. Chem. B*, 1997, **101**, 4925.
24 J. S. Kim, S. C. Yang and B. S. Bae, *J. Sol-Gel Sci. Technol.*, 2009, **53**, 434.
25 Y. J. Eo, J. H. Kim, J. H. Ko and B. S. Bae, *J. Mater. Res.*, 2005, **20**, 401.
26 D. R. Bauer and G. F. Budde, *Ind. Eng. Chem. Prod. Res. Dev.*, 1981, **20**, 674.
27 G. Montaudo, M. S. Montaudo, C. Puglisi and F. Samperi, *Macromolecules*, 1995, **28**, 4562.
28 S. Icanocici and G. Kickelbick, *J. Sol-Gel Sci. Technol.*, 2008, **46**, 273.
29 W. L. Robb, *Ann. N. Y. Acad. Sci.*, 1968, **146**, 119.
30 M. W. Simon, K. T. Stafford and D. L. Ou, *J. Inorg. Organomet. Polym. Mater.*, 2008, **18**, 364.